БЪЛГАРСКА АКАДЕМИЯ НА НАУКИТЕ • BULGARIAN ACADEMY OF SCIENCES
АСТРОФИЗИЧЕСКИ ИЗСЛЕДВАНИЯ, 7 • ASTROPHYSICAL INVESTIGATIONS, 7
София • 1996 • Sofia

Scanning of stellar images by a slit diafragm and estimation of their parameters. II. Smoothing of stellar images having a quasi-Gaussian intensity distribution

D. V. Dimitrov

A B S T R A C T

The distortions due to the scanning of stellar images with a quasi-Gaussian intensity distribution ($\sim \exp(-r^{2n_c}/B)$) by a slit diafragm are investigated.It is assumed a constant value of the power n_c .The smoothed by the diafragm intensity distribution is again approximated by a function of the same kind,but the power $\tilde{n}(x)$ in this case depends on the slit position with respect to the center of the image.There is also dependence on the slit width $2h$ (in units of the stellar image size σ ; $B=(2\sigma^2)^{n_c}$).We analyze the relation between $\tilde{n}(x)$ and n_c by means of analytical expressions and numerical methods. The results are presented graphically.

Key words: stellar images,scanning,approximation.

I. Introduction

Knowledge of the intensity distribution within the long-exposure stellar images has important consequences for the precise photometrical study of the astronomical objects. The solution of this task is also valuable when a reconstruction of extended images is applied.In many cases this intensity distribution is well fitted (in a first-order approximation) by a Gaussian function.Nevertheless,there is a sense to attempt for such purposes other functional approximations in order to improve the fitting. In general, we expect that the extention of the fitting will include an additional number of parameters. The appropriateness of the new generalized approximation depends on the possibility to measure the introduced parameters and to evaluate accuratelly their errors. In this paper we investigate a quasi-Gaussian distribution, where the power of the argument of the exponential function is not fixed equal to 2, as in the case of a Gaussian distribution, but is allowed to vary within given limits.

Let us introduce in the focal plane of the telescope (or in the plane of the plate, if photographic images are scanned) a Cartesian coordinate system (x, y) . Its origin is set to coincide with the center of the smeared stellar image under consideration. We suppose also that these long-exposure images are not elongated due to the badly guiding or to the atmospheric dispersion. Therefore, the measured intensity distribution is determined only by the radial distance from the center of the image $r \equiv (x^2+y^2)^{1/2}$. The investigated in this paper distribution is given by

$$(1) \quad g(x,y) \equiv g(r) = S \exp\left(-r^{2n}/B\right) \equiv S \exp\left[-\left(r^2/2\sigma^2\right)^n\right]$$

where S is a normalization constant related to the total flux in the image and $B \equiv (2\sigma^2)^n$ characterises the size of the image. The power n is a new parameter. Its difference from unity describes the difference of $g(r)$, given by (1), from the Gaussian curve for which $n \equiv 1$. It would be notted that the changes of n affect mainly the slope of the curve $g(r)$, but have a little influence on its width. It would also be emphasized that

σ and n are independent parameters, and the expression (1) is a 3-parametric curve, depending not only on the space coordinate τ, but also on the parameters S, σ and n. Obviously, in the particular case of a Gaussian distribution, n is a constant equal to 1, and σ^2 is the dispersion. If n = const, but is not equal to 1, $\sqrt{2}\,\sigma$ gives the radial distance from the center of the image at which the intensity drops to e^{-1} = 36.8 % from the central value (like the Gaussian case).

II. Definition of the problem

If n does not depend on τ, there is no difficulty to express this quantity through $g(\tau)$ and its derivatives $g'(\tau)$ and $g''(\tau)$, where the prime's denote differentiating with respect to τ. For this purpose we may take the natural logarithms from the two sides of (1), and after differentiating with respect to τ, we have

$$(2) \qquad -\frac{g'(\tau)}{g(\tau)} = \frac{2n}{B}\tau^{2n-1} \geq 0 \quad ; n = \text{const}.$$

Both sides of the above expression are positive for $\tau > 0$ and we may again take the natural logarithms from the left and right hand sides of (2), and differentiate with respect to τ. The final expression for n is (Dimitrov, 1980a)

$$(3) \qquad n = 0.5\left[1 + \tau\left(\frac{g''(\tau)}{g'(\tau)} - \frac{g'(\tau)}{g(\tau)}\right)\right] = \text{const}.$$

It would be stressed that in the above computations we have essentially used the basic assumption that the power n does not depend on τ. Strictly speaking, the theoretical investigations of the intensity distribution within the turbulent stellar images show that n may be not only smaller than unity, but also depends on τ (Dimitrov, 1980b). An analogical situation when $n \neq$ const may arise also when photographical images are approximated by the quasi-Gaussian curve (1). Our intention is to investigate the smoothing effect on the distribution (1) caused by the scanning procedure. Throughout this paper we are dealing with an infinitely long slit diafragm aligned to the axis y. The slit has a finite width $2h$. Further, the abscissa of the middle line (parallel to axis y) of the slit is denoted by x. Then the transmitted through the diafragm energy flux is given by (Dimitrov, 1980a)

$$(4) \quad 2h\tilde{g}(x) = S\int_{x-h}^{x+h}\left\{\left[\int_{-\infty}^{\infty}\exp\left[-\frac{(x_1^2+y^2)^n}{B}\right]dy\right]\right\}dx_1,$$

where $\tilde{g}(x)$ is the smoothed by the slit diafragm quasi-Gaussian distribution (1).

Let us approximate $\tilde{g}(x)$, by analogy with $g(\tau)$, by a quasi-Gaussian curve of the same kind as the distribution (1)

$$(5) \quad \tilde{g}(x) = \tilde{S}\exp\left(-x^{2\tilde{n}}/\tilde{B}\right) \equiv \tilde{S}\exp\left[-\left(x^2/2\tilde{\sigma}^2\right)^{\tilde{n}}\right];$$
$$\tilde{B} \equiv \left(2\tilde{\sigma}^2\right)^{\tilde{n}},$$

where the tilde's denote quantities related to the smoothed distribution. What may be said about the parameters $\tilde{S}$, $\tilde{\sigma}$ and $\tilde{n}$ with respect to their unsmoothed values S, σ and n, respectively? The scanning does not change the total energy flux from the image, but slightly enlarges its width and decreases its central intensity, correspondingly. Consequently, $\tilde{S} < S$. For

Gaussian curves, this increasing of $\tilde{\sigma}$ relative to σ is of the order of ~ 1 % (Dimitrov, paper in this volume). There is not reason to believe that the situation is essentially distinct in the non-Gaussian case ($n \neq 1$), provided that n is not too different from unity. Because we are not interesting now of the total flux, the only remaining parameter which we shall investigate in this work is the quantity $\tilde{n}$, describing the variation of the slope of the function $\tilde{g}(x)$. In general, we may expect that $\tilde{n}$ depends on the position of the scanning slit x, even if n is a constant. According to (4), the smoothed curve $\tilde{g}(x)$ represents an averaging of $g(r=\sqrt{x^2+y^2})$ over the diafragm area. Nevertheless, the scanning along the axis x, with a consequent using of the approximation (5), gives a (distorted) local estimation $\tilde{n}$ for the quantity n. We may use the scanning data in an attempt to evaluate $\tilde{n} = \tilde{n}(x)$ by means of a relation which is an analogy to the formula (3)

$$(6) \quad \tilde{n}(x) = 0.5 \left[1 + x \left(\frac{\tilde{g}''(x)}{\tilde{g}'(x)} - \frac{\tilde{g}'(x)}{\tilde{g}(x)} \right) \right] ;$$

($x \geq 0$ and locally $\tilde{n}$ = constant),

where the prime's denote differentiating of the smoothed curve $\tilde{g}(x)$ with respect to x. It would be noted that the application of (6) to the data does not require knowledge of the parameters $\tilde{S}$ and $\tilde{B} = (2\tilde{\sigma}^2)^{\tilde{n}}$, but the center of the image must be preliminary known (because we have set the abscissa of the center of the image x_0 to be equal to zero).

Generally speaking, there are two distinct reasons for to depend on x :

(i) The intrinsic variability of the undisturbed by the scanning power $n = n(\tau = \sqrt{x^2 + y^2})$ (Dimitrov, 1980b). It is suitable to measure this functional dependence by a circular diafragm with a radius well bellow the size of the stellar image σ ,but not by a slit diafragm which may have a width $2h$ comparable to σ. This source of global variability is fully neglected in the present work. Throughout this paper it is assumed that the quantity n has a constant global value n_c ,which to some extent is an averaged over to whole stellar image mean value of the function $n(\tau)$;

(ii) According to (4), the total intensity transmitted through the slit is a linear superposition of the intensities from different points of the image, which are not the same as the intensity at the point (x,y = 0). Consequently, the smoothed distribution $\tilde{g}(x)$ is characterized by a power $\tilde{n}$,different from n_c ,and depending on x even if n_c = constant. Because the slit is perpendicular to the axis x ,we expect that the points near the abscissa give the main contribution to the total transmitted flux. In that sense, routhly speaking, $\tilde{g}(x)$ represents a "radially" smoothed distribution of the unperturbed quasi-Gaussian function $g(\tau = x, y \equiv 0)$ (1). For this reason, we have adopted formula (6), by analogy with (3), to compute the global changes of the local (slit averaged) values of $\tilde{n}(x)$.

It would be mentioned that the presence of the second derivative $\tilde{g}''(x)$ in the expression (6) requires using of a wider slit diafragm in order to measure $\tilde{g}(x)$ with a high enough signal to noise ratio (the derivatives $\tilde{g}'(x)$ and $\tilde{g}''(x)$ are numerically computed from $\tilde{g}(x)$). This obstacle introduces larger smoothing of the parameters S , σ and exceptionally n .

In the next sections of this paper we give a quantitative evaluation of the differences between $\tilde{n}(x)$ and n_c = const , depending on the slit width $2h$.

III. Analytical expressions

According to our preceeding assumptions we set into (4) $n = n_c$ = const and S = 1. The later equality is introduced because we are not interesting on the total flux, but only on the slope of the distribution $\tilde{g}(x)$. Taking into account that the stellar image is symmetric with respect to axis x , the integration over y may be performed only from zero to infinity, and (4) can be rewritten as

$$\tilde{g}(x) = h^{-1}\int_{-\infty}^{x+h}\left\{\int_0^{\infty}\exp\left[-(x_1^2+y^2)^{n_c}/B\right]dy\right\}dx_1 - h^{-1}\int_{-\infty}^{x-h}\left\{\int_0^{\infty}\exp\left[-(x_1^2+y^2)^{n_c}/B\right]dy\right\}dx_1 . \tag{7}$$

Differentiating the above expression with respect to x one or two times, we obtain analytical results for the first $\tilde{g}'(x)$ and second $\tilde{g}''(x)$ derivatives, respectively

$$\tilde{g}'(x) = h^{-1}\int_0^{\infty}\exp\left\{-\frac{\left[(x+h)^2+y^2\right]^{n_c}}{B}\right\}dy - h^{-1}\int_0^{\infty}\exp\left\{-\frac{\left[(x-h)^2+y^2\right]^{n_c}}{B}\right\}dy ; \tag{8}$$

$$\tilde{g}''(x) = -\frac{2n_c}{hB}\Bigg[\!\!\Bigg[(x+h)\int_0^\infty \left[(x+h)^2+y^2\right]^{n_c-1} \times \exp\left\{-\left[(x+h)^2+y^2\right]^{n_c}/B\right\}dy - (x-h)\int_0^\infty \left[(x-h)^2+y^2\right]^{n_c-1} \times \exp\left\{-\left[(x-h)^2+y^2\right]^{n_c}/B\right\}dy\Bigg]\!\!\Bigg]. \tag{9}$$

a) Scanning of stellar images vaving an exact Gaussian distribution by an infinitely thin slit ($n_c = 1, h \ll \sigma$)

Let us denote by $\mathcal{K}$ the constant

$$\mathcal{K} = \int_0^\infty \exp\left(-y^2/B\right) dy. \tag{10}$$

We set $n_c = 1$ in the formulae (7) - (9) and use the L'Hospital's rule for evaluation of indeterminate expressions in terms of the ratio 0/0 in order to perform the transition $h \to 0$. Because in (6) we are involved only the ratios of the functions $\tilde{g}(x)$, $\tilde{g}'(x)$ and $\tilde{g}''(x)$,without loosing of generality we set further $S = 1$.

$$\lim_{h\to 0} \tilde{g}(x) = \lim_{h\to 0} \frac{\left[h\tilde{g}(x)\right]}{h} = \lim_{h\to 0} \frac{d}{dh}\left[h\tilde{g}(x)\right] = 2\mathcal{K}\exp\left(-x^2/B\right) ; \tag{11}$$

$$\lim_{h\to 0}\tilde{g}'(x) = \lim_{h\to 0}\frac{[h\,\tilde{g}'(x)]}{h} = \lim_{h\to 0}\frac{d}{dh}\left[h\,\tilde{g}'(x)\right] \tag{12}$$

$$= -\frac{2\mathcal{K}}{B}\lim_{h\to 0}\Big\{(x+h)\exp\left[-(x+h)^2/B\right]$$

$$+ (x-h)\exp\left[-(x-h)^2/B\right]\Big\}$$

$$= -\frac{4\mathcal{K}}{B}\,x\,\exp(-x^2/B)\ ;$$

$$\lim_{h\to 0}\tilde{g}''(x) = -\frac{2\mathcal{K}}{B}\lim_{h\to 0}\Big\{h^{-1}(x+h) \tag{13}$$

$$\times\exp\left[-(x+h)^2/B\right] + h^{-1}(x-h)\exp\left[-(x-h)^2/B\right]\Big\}$$

$$= -\frac{4\mathcal{K}}{B}\left(1-2x^2/B\right)\exp(-x^2/B)\ .$$

From (11) - (13) it follows

$$\tilde{g}''(x)/\tilde{g}'(x) = x^{-1} - 2x/B\ , \tag{14}$$

and

$$\tilde{g}'(x)/\tilde{g}(x) = -2x/B\ , \tag{15}$$

where there is not need to compute the constant $\mathcal{K}$ from (10). From the above two equalities it obviously follows, according to (6), that the smoothed value of the power $\tilde{n}(x)$ is exactly equal to unity constant, independent of x. Consequently, when images with a Gaussian distribution of the intensity are scanned by a narrow infinitely long slit, the resulting distribution is again a Gaussian one ($\tilde{n}(x) \equiv 1$) with the same dispersion σ^2 (Dimitrov, paper in this volume). Intuitively, we should expect that the situation with the slope of the smoothed curve is not different in the case when $n(x)$ is close to unity, but the quantitative check of this statement requires numerical calculations, as it is done in the next section.

b) Scanning of stellar images having an exact Gaussian distribution by a slit with a width $2h$ comparable to the size of the image σ ($n_c = 1$, $2h \gtrsim \sigma$)

Let us compute the integral

$$L(z)=\int_0^\infty \exp\left(-\frac{y^2+z^2}{B}\right)dy=\exp\left(-\frac{z^2}{B}\right)\int_0^\infty \exp\left(-\frac{y^2}{B}\right)dy, \tag{16}$$

or

$$L(z)=\frac{\sqrt{\pi B}}{2}\exp\left(-z^2/B\right) . \tag{17}$$

We can express $\tilde{g}(x)$, $\tilde{g}'(x)$ and $\tilde{g}''(x)$ through the function $L(z)$. Substituting $n_c = 1$ in the formulae (7) - (9) we have

$$\tilde{g}(x)=h^{-1}\int_{x-h}^{x+h} L(x_1)dx_1=\frac{\sqrt{2\pi}\,B}{4h}\int_{\sqrt{2}(x-h)/\sqrt{B}}^{\sqrt{2}(x+h)/\sqrt{B}} \exp\left(-x_1^2/2\right)dx_1. \tag{18}$$

Finally, we get the following expression for the smoothed curve $\tilde{g}(x)$

$$\tilde{g}(x)=\frac{\pi B}{2h}\left\{\Phi\left[\sqrt{2}(x+h)/\sqrt{B}\right] - \Phi\left[\sqrt{2}(x-h)/\sqrt{B}\right]\right\}, \tag{19}$$

where $\Phi(x) = (2\pi)^{-1/2} \int_{-\infty}^{x} \exp(-t^2/2)\, dt$ is the error integral (Korn et al., 1977). Further, from (8) we have

$$(20) \quad \tilde{g}'(x) = h^{-1} \left[\mathcal{K}(x+h) - \mathcal{K}(x-h) \right]$$

$$= \frac{\sqrt{\pi B}}{2h} \left\{ \exp\left[-\frac{(x+h)^2}{B} \right] - \exp\left[-\frac{(x-h)^2}{B} \right] \right\}.$$

Correspondingly, from (9) follows that

$$(21) \quad \tilde{g}''(x) = -(2/hB) \left[(x+h)\mathcal{K}(x+h) - (x-h)\mathcal{K}(x-h) \right]$$

$$= (\sqrt{\pi}/h\sqrt{B} \left\{ (x-h) \exp\left[-(x-h)^2/B \right] - (x+h) \exp\left[-(x+h)^2/B \right] \right\}.$$

The error integral $\Phi(x)$ is tabulated in many reference books (Abramowitz et al., 1979, chapter 7 ; Janke et al., 1977 ; Korn et al., 1977). There are also analytical expressions for its calculation (Abramowitz et al., 1979, chapter 7). Therefore, the expressions (19) - (21) enable us to calculate analytically the local values of the smoothed power $\tilde{n}(x)$ by setting them into formula (6). The results $\tilde{n}(x)$ are listed in Table 1 (first rows) for $n_c = 1$ and $\sigma = 1$ (e.g., $B = 2$). The width of the slit $2h$ varies from 0.30 to 2.50 (in units $\sigma = 1$). It is evident that $\tilde{n}(x)$ is at some extent larger than the unsmoothed value $n_c = 1$ if the width of the slit $2h$ is comparable to the diameter of the stellar image 2σ. The enlargement is more pronounced when the outer parts of the images are scanned and may reach the order of a few per cent.But it would be emphasized that the scanning procedure gives here not very good signal to noise ratio in comparision to the central parts of the images.We may expect that a such enlargement of the smoothed powers $\tilde{n}(x)$ will be seen in the cases when $n_c \neq 1$. This can be understood in the following way.The smaller values of the power n in the expression (1) mean that its central part (giving the main contribution into the flux) is sharper.The scanning of the image flattens its shape and , consequently,we expect that the smoothed power $\tilde{n}$ is larger.This qualitative treatment is checked in the next section (Fig.1 a-i).

IV. Numerical evaluations ($n_c \leq 1$)

Computing of the smoothed values of the power $\tilde{n}(x)$ requires numerical integrations of the expressions (8) and (9).In view of the fact that the turbulent stellar images have an intrinsic (variable) power $n(r)$ less than unity (Dimitrov,1980b,Fig.2),we have considered only (constant) unsmoothed powers n_c also less than unity: n_c = 0.55,0.60,...,0.95 and 1.00.It would be noted that the numerical integration of $\tilde{g}'(x)$ (eq.(8)) and $\tilde{g}''(x)$ (eq.(9)) must be performed only by one Cartesian coordinate y . For the expression (7) a similar numerical integration (in that case by two Cartesian coordinates x_1 and y) is more tedious. Of course,the expression (7) for $\tilde{g}(x)$ may be simplificated if instead of Cartesian coordinates (x_1, y) polar coordinates (r ,θ) are used.In the later case it is possible to perform an analytical integration over the polar angle θ ,and then it remains to integrate over r numerically.In the case of polar coordinates (r , θ) it may be shown that instead of (7) we can use the expressions ($\mathcal{S}$ = 1)

$$\text{(22)}\quad \tilde{g}(x) = \pi h^{-1}\int_0^\infty \tau \exp\left(-\tau^{2n_c}/B\right) d\tau$$

$$- h^{-1}\int_0^\infty \tau \arccos\left(\frac{h-x}{\tau}\right)\exp\left(-\tau^{2n_c}/B\right) d\tau$$

$$- h^{-1}\int_{x+h}^\infty \tau \arccos\left(\frac{x+h}{\tau}\right)\exp\left(-\tau^{2n_c}/B\right) d\tau \quad ,$$

for $x \leq h$, and

$$\text{(23)}\quad \tilde{g}(x) = h^{-1}\int_{x-h}^\infty \tau \arccos\left(\frac{x-h}{\tau}\right)\exp\left(-\tau^{2n_c}/B\right) d\tau$$

$$- h^{-1}\int_{x+h}^\infty \tau \arccos\left(\frac{x+h}{\tau}\right)\exp\left(-\tau^{2n_c}/B\right) d\tau \quad ,$$

for $x \geq h$.

But even this method of numerical integration over τ , with a view to obtain $\tilde{g}(x)$,requires more computations in comparision with the direct numerical integration of the derivative $\tilde{g}'(x)$ .We here suppose that the derivative $\tilde{g}'(x)$ is already computed from the analytical expression (20).Because (20) and (21) are analytical formulae,the term "numerical" in our method means that we only perform a numerical integration over of the function $\tilde{g}'(x)$ .The constant of integration was found from the condition $\tilde{g}(\infty)$ = 0.This integration constant would not be mistaken with the normalization constant $\mathcal{S}$ which was already been set equal to unity in the expressions (7) - (9).The computed values of $g(x)$, $\tilde{g}'(x)$ and $\tilde{g}''(x)$ for x ranging from 0.0 to 3.0 (in units σ = 1) were used for evaluation of $\tilde{n}(x)$ according to formula (6).The results are expressed in Fig.1 a-i ,and for the Gaussian case (n_c = 1) in Table 1 (second rows).In all cases we have set $\sigma = 1$ (respectively, $B = 2^{n_c}$).

V. Discussion

From Fig.1 a-i it is evident that the finite width of the slit diafragm causes an increasing of the power $\tilde{n}(x)$ relatively to the unsmoothed constant value n_c .This is more clearly manifested for the central ranges of the scanned stellar images. This circumstance is an essential deficiency of a such kind of measurements of the intensity distribution,because here is concentrated the dominant part of the light flux.As would be expected,if the slit width $2h$ is greater,the greater are the distortions of the power n .It is evident the tendency of their sharp increasing when $2h$ becomes of the order or even greater than σ .Moreover,when the difference $|n_c - 1|$ is larger, the larger is the distinction between $\tilde{n}(x)$ and n_c .

In the Gaussian case $n_c = 1$,the results obtained by the numerical integration are compared with the results obtained by the analytical expressions (6),(18) - (21) (Table 1,second and first rows,respectively).The agreement between these values is satisfied with the exeption of $x \gtrsim 3.0$.The discrepancies are due to the insufficient accuracy of the numerical integration at large x .In that case the distribution $\tilde{g}(x)$ is obtained by the numerical integration of $\tilde{g}'(x)$

$$\tilde{g}(x)=\int_0^{\infty}\tilde{g}'(x_1)dx_1+C_1\approx\sum_{i=0}^{\ell}\tilde{g}'(x_i)\Delta x+C_1\,, \tag{24}$$

where C_1 is an integration constant, Δx is the step of the integration, $x_0 = 0$,and $x_\ell = x$ .A small inaccuracy arising during the procedure of the numerical integration (24) may lead to a certain inaccuracy in deriving of the constant C_1 when the boundary condition

(25) $$\lim_{x \to \infty} \tilde{g}(x) = 0$$

is used. A systematic underestimation of C_1 arises from the impossibility to perform the numerical integration in (24) strictly to $x = +\infty$ in order to compute C_1 from (25). Consequently, the values of $\tilde{g}_{num}(x)$ may be turned out to be lower by a constant value. For large x, $\tilde{g}(x)$ is close to zero, and the reduce of leads to the overestimate of the ratio $\tilde{g}'(x)/\tilde{g}(x)$, and according to (6), to the overestimation of $\tilde{n}(x)$.

In the quasi-Gaussian case ($n_c < 1$), it may be seen that for $x > \sigma$, $\tilde{g}(x)$ will decrease (with the increasing of x) more slowly than when $n_c = 1$, and this slow down is more pronounced for n_c more different from unity. Consequently, for smaller n_c the erroneousness of the integration constant C_1 (and respectively, of $\tilde{g}(x)$ at large x) will also be smaller. According to Table 1, the accuracy of the numerical integration is checked in comparison with the analytical method for the Gaussian case $n_c = 1$. Taking into account the above considerations, we are certain that the graphic results presented in Fig. 1 a-i are realible for $x \lesssim 2.8$.

Instead of the boundary condition at infinity (25), we are able to use another boundary condition when the slit diafragm is placed at the center of the stellar image $x = 0$. Remembering that we already have assumed $\sigma = S = 1$, from (22) follows an analytical expression for $\tilde{g}(x=0)$

(26) $$C_2 \equiv \tilde{g}(0) = \pi k^{-1} \int_0^\infty r \exp(-r^{2n_c}/B)\, dr$$

$$-2h^{-1}\int_h^{\infty} r \arccos(h/r)\exp(-r^{2n_c}/B)\,dr$$

$$=\frac{\pi B^{1/n_c}}{2n_c h}\Gamma\left(\frac{1}{n_c}\right)-2h^{-1}\int_h^{\infty} r\arccos(h/r)\exp(-r^{2n_c}/B)\,dr,$$

where $B^{1/n_c} = 2$ and $\Gamma(1/n_c)$ is the Gamma function with argument $1/n_c$ .Consequently,instead of (24),we may use the numerical evaluation

$$\tilde{g}(x)=\int_0^x \tilde{g}'(x_1)\,dx_1+C_2 \approx \sum_{i=0}^{\ell} \tilde{g}'(x_i)\Delta x + C_2 , \tag{27}$$

where C_2 is computed from (26).Of course,if we were able to evaluate C_1 and C_2 accurately,we should obtain $C_1 = C_2$ .It is evident that the accuracy of determination of the constant C_2 is not affected by the integration of $\tilde{g}'(x)$ over x and depends only on the numerical evaluation of the integral in the right--hand side of (26).

If the expression (27) is used to compute $\tilde{g}(x)$,than the inaccuracities will be accumulated at large x .In the opposite case,the estimate of the constant C_1 has accumulated all errors during the numerical integration of $\tilde{g}'(x)$ from 0 to infinity. Consequently,the increasing of x in (24) will lead to an increasing compensation of the error of the constant C_1 .In spite of that,the equation (27) gives a more exact estimation for $x \approx 0$; here $\tilde{g}(x)$ is close to its maximal value, $\tilde{g}'(x)$ is close to zero, and consequently,the ratio $\tilde{g}'(x)/\tilde{g}(x)$ does not depend strongly on the error of $\tilde{g}(x)$ .We prefered to use the value of C_1 instead that of C_2 .

It would also be noted that if the functions $\tilde{g}(x)$, $\tilde{g}'(x)$ and $\tilde{g}''(x)$ are simultaneously increased (or reduced) because of the finite integration step Δx , this will not affect on $\tilde{n}(x)$.

VI. Conclusions

In this paper we have considered stellar images with a circular quasi-Gaussian unsmoothed intensity distribution $g(r) \sim \exp(-r^{2n_c}/B)$, where the power n_c has a global (for the whole area of the image) constant value. It is investigated the smoothing effect on this parameter when the images are scanned by an infinitely long slit with a finite width $2h$. In all cases the transmitted flux again may be approximated by a quasi-Gaussian distribution of the same kind, but the "observed" power $\tilde{n}$ depends on the position of the slit and has always values greater than n_c (for reasonable values of the ratio $2h/\sigma$). The numerically computed relations between $\tilde{n}(x)$ and n_c (for a preliminary known value of $2h/\sigma$) may be used to correct the measured $\tilde{n}(x)$'s in order to obtain the unsmoothed power n_c . As can be seen from Fig. 1 a-i , $\tilde{n}(x)$ is close to unity at the center of the images, increases to a maximal value (if $1.00\ h/\sigma \lesssim x \lesssim 1.25\ h/\sigma$) and for large x tends to n_c . At first glance, it may be suggested that it is better to evaluate n_c from scans made far from the center of the image. However, it would be stressed that, according to (6), we must evaluate from the data not only the first derivative $\tilde{g}'(x)$, but also the second derivative $\tilde{g}''(x)$. To obtain a better accuracy, this leads to the necessity to use a larger slit width $2h/\sigma$ (which gives a better signal to noise ratio), and consequently, to enlarge the difference $\tilde{n}(x) - n_c$.

In the opposite case, when the central parts of the images are scanned, it may arise another difficulty, which is not considered in this paper. For a real-time photoelectrically scanned turbulent stellar disks, the power n has not a constant value n_c and varies rapidly with respect to τ at the center of the images (Dimitrov, 1980b, Fig. 2). Moreover, even if n_c = constant for $x \gtrsim 0$, as follows from Fig. 1 a-i, the smoothed values $\tilde{n}(x)$ are very close to unity, independently of the fact how different is n_c from unity. This leads to a greate ambiguity in the restoration of the original values of n_c, unsmoothed by the slit diafragm. Therefore, instead of the obstacle that the differences $\tilde{n}(x) - n_c$ are large at the "middle" parts of the images (Fig. 1; $0.5\,\sigma \lesssim x \lesssim 2.5\,\sigma$), it is preferable to use just this range of the scans, because the corrections $\tilde{n}(x) - n_c$ may be determined with a relatively sufficient accuracy.

References

Abramowitz, M., Stegun, I.A. 1979. Handbook of Mathematical Functions with Formulas, Graphs and Mathematical Tables. 'Nauka' Publ. House, Moscow.

Dimitrov, D.V. 1980a. Vestnik K'harkov. Univ. No 204, p.44.

Dimitrov, D.V. 1980b. Vestnik K'harkov. Univ. No 204, p.40.

Dimitrov, D.V. Astrophysical Investigations, 7 (this volume).

Janke, E., Emde, F., Losch, F. 1977. Special Functions. 'Nauka' Publ. House, third edition, Moscow.

Korn, G.A., Korn, T.M. 1977. Mathematical Handbook for Scientists and Engineers. 'Nauka' Publ. House, 4 th edition, Moscow.

Address: Space Research Institute of the Bulgarian Academy of Sciences, 6 Moscowska str., 1000 Sofia, P.O. 799, Bulgaria

Table 1

Comparison between analytically (first rows) and numerically (second rows) computed smoothed values of the power $\tilde{n}(x)$;

Gaussian case: $n_c = 1.00$; $B = 2$ ($\sigma = 1$)

	$\tilde{n}(x)$					
x \ $2h$	0.30	0.60	1.00	1.40	2.00	2.50
0.2	1.000	1.000	1.000	1.000	1.001	1.002
	1.000	0.998	1.000	0.999	1.000	1.001
0.4	1.000	1.000	1.000	1.001	1.003	1.008
	1.000	0.999	0.999	1.000	1.003	1.007
0.6	1.000	1.000	1.000	1.002	1.007	1.016
	0.999	0.999	1.000	1.001	1.006	1.015
0.8	1.000	1.000	1.001	1.003	1.012	1.027
	0.999	0.999	1.000	1.002	1.011	1.026
1.0	1.000	1.000	1.001	1.005	1.018	1.039
	0.999	0.999	1.000	1.004	1.017	1.038
1.2	1.000	1.000	1.002	1.007	1.024	1.052
	0.999	0.999	1.001	1.006	1.023	1.051
1.5	1.000	1.000	1.003	1.010	1.033	1.069
	0.999	0.999	1.002	1.009	1.033	1.067
1.8	1.000	1.000	1.004	1.013	1.042	1.083
	1.000	0.999	1.003	1.013	1.042	1.082
2.1	0.999	1.001	1.005	1.016	1.050	1.093
	1.002	1.004	1.007	1.017	1.050	1.093
2.4	1.004	1.002	1.006	1.019	1.056	1.100
	1.011	1.014	1.015	1.026	1.060	1.101
2.7	1.000	1.000	1.008	1.022	1.060	1.105
	1.035	1.047	1.045	1.050	1.079	1.115
3.0	0.992	0.999	1.009	1.026	1.063	1.107
	1.214	1.176	1.159	1.149	1.119	1.133

Figure Captions

Fig.1 a-i .Dependence of the smoothed power $\tilde{n}(x)$ vs. the infinite slit position. Thin solid lines: h/σ = 0.15 ; thin dashed lines: h/σ = 0.30 ; dotted lines: h/σ = 0.50 ; dash-dotted lines: h/σ = 0.70 ; thick solid lines: h/σ = 1.00 ; crosses: h/σ = 1.25 .

a - n_c= 0.55 ; b - n_c= 0.60 ; c - n_c= 0.65 ; d - n_c= 0.70 ;

e - n_c= 0.75 ; f - n_c= 0.80 ; g - n_c= 0.85 ; h - n_c= 0.90 ;

i - n_c= 0.95 . In each case the straight thick dashed line indicates the corresponding unsmoothed constant global value of n_c

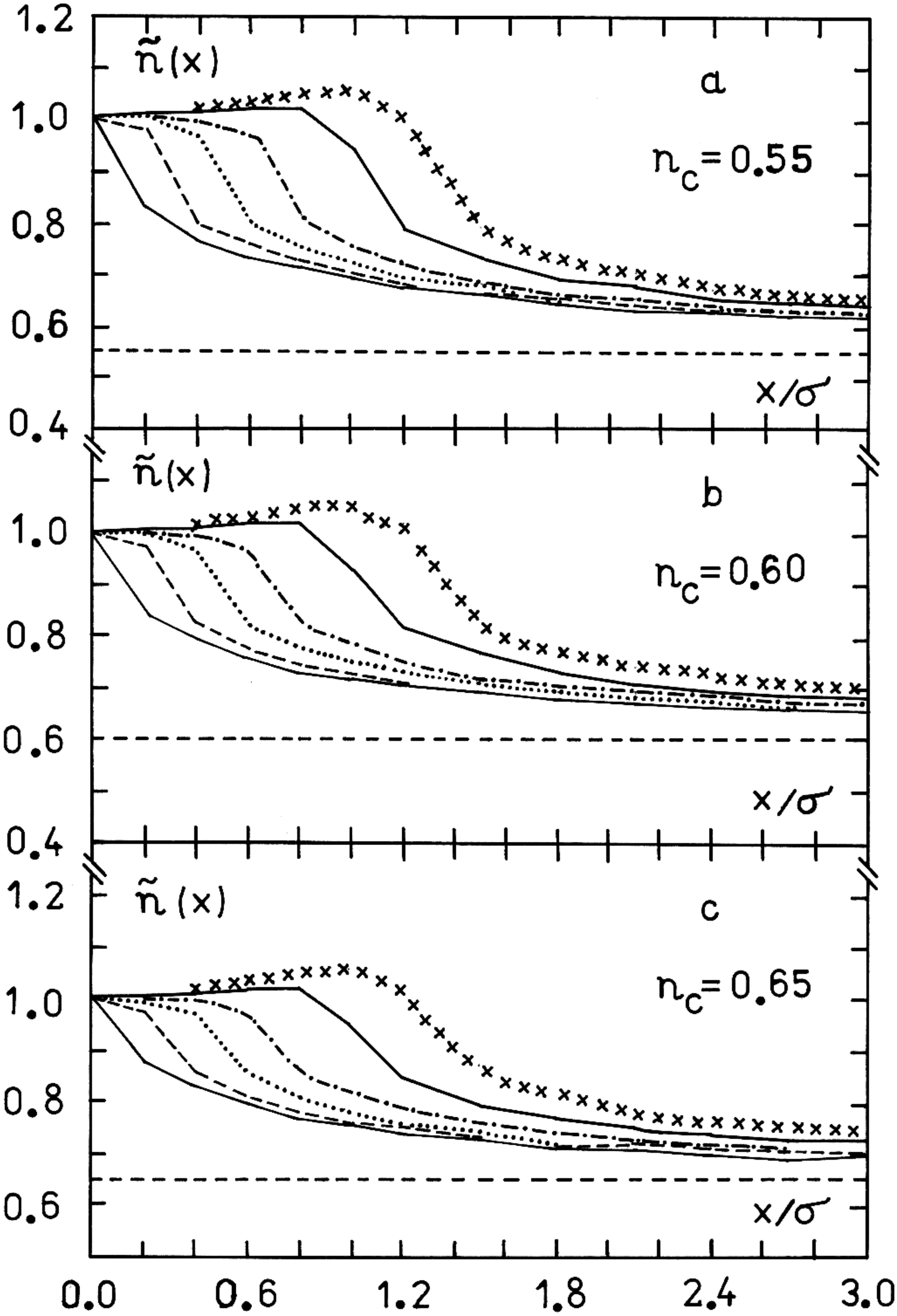

1.2
$\tilde{n}(x)$
a
1.0
$n_c = 0.55$
0.8
0.6
x/σ
0.4
$\tilde{n}(x)$
b
1.0
$n_c = 0.60$
0.8
0.6
x/σ
0.4
1.2
$\tilde{n}(x)$
c
1.0
$n_c = 0.65$
0.8
0.6
x/σ
0.0
0.6
1.2
1.8
2.4
3.0

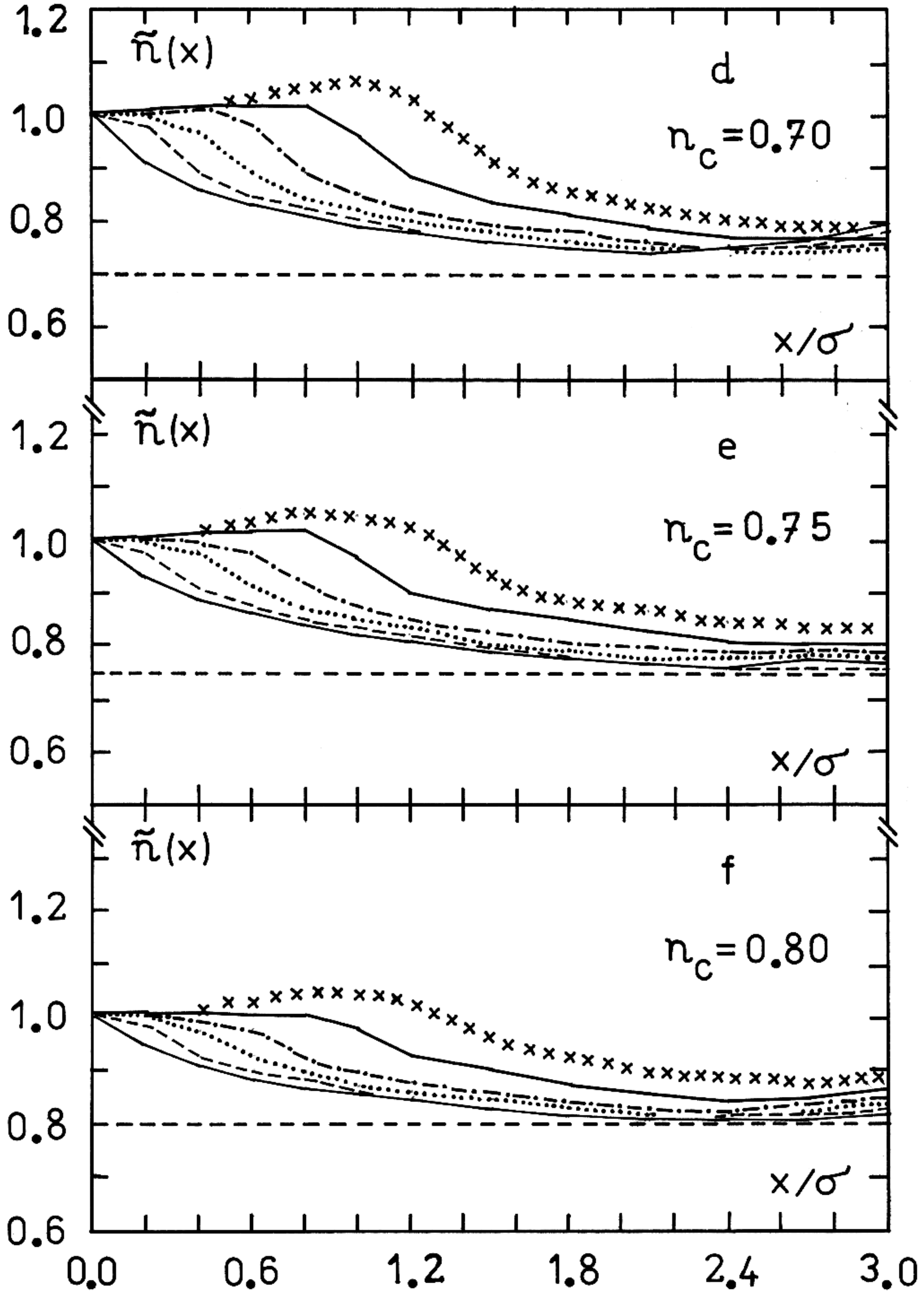

1.2
1.0
0.8
0.6
ñ(x)
d
n_c=0.70
x/σ
1.2
1.0
0.8
0.6
ñ(x)
e
n_c=0.75
x/σ
1.2
1.0
0.8
0.6
ñ(x)
f
n_c=0.80
x/σ
0.0
0.6
1.2
1.8
2.4
3.0

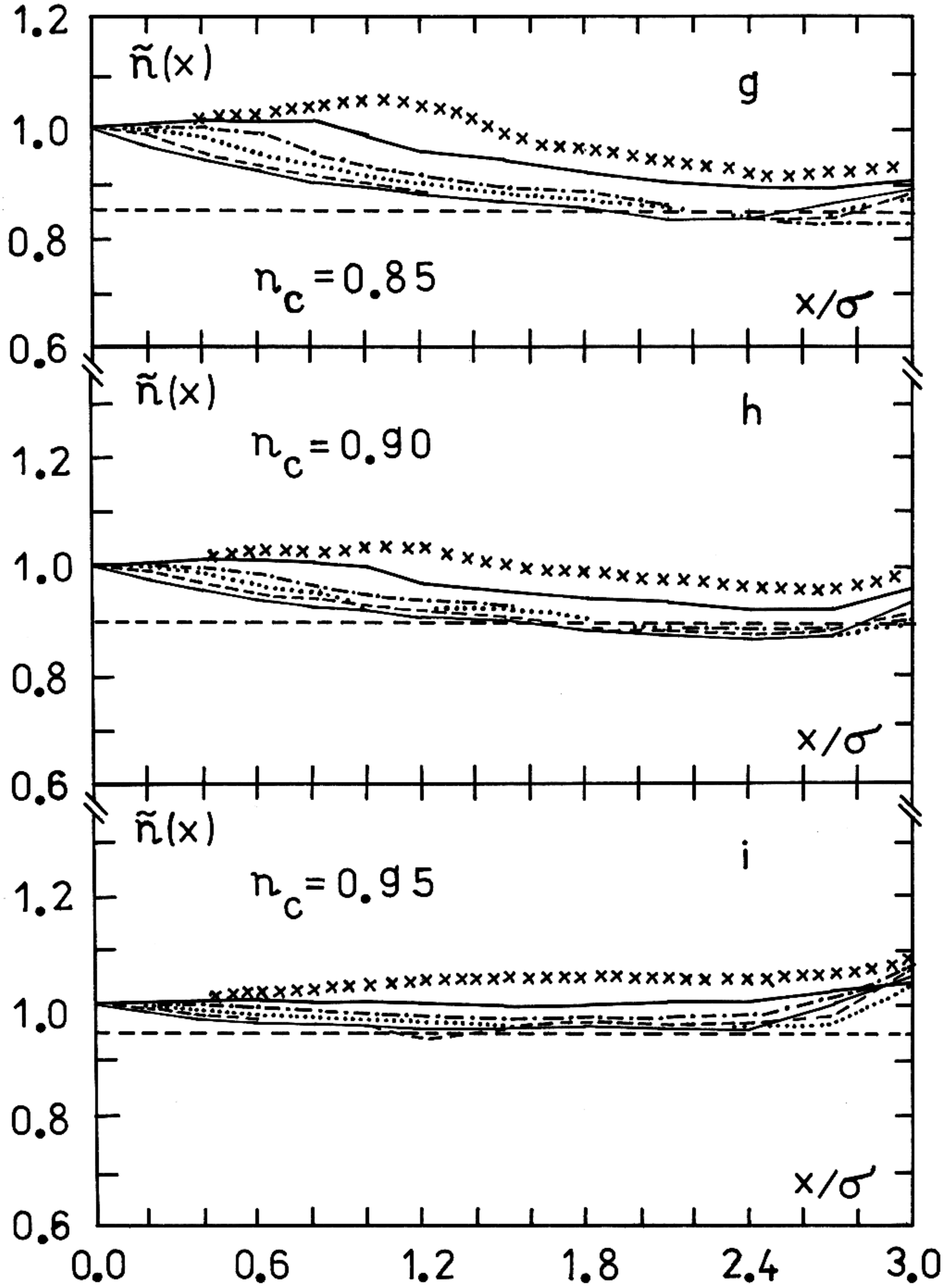
1.2
$\tilde{n}(x)$
g
1.0
0.8
$n_c = 0.85$
x/σ
0.6
$\tilde{n}(x)$
h
$n_c = 0.90$
1.2
1.0
0.8
x/σ
0.6
$\tilde{n}(x)$
i
$n_c = 0.95$
1.2
1.0
0.8
x/σ
0.6
0.0
0.6
1.2
1.8
2.4
3.0